Targeted nanotherapy with everolimus reduces inflammation and fibrosis in scleroderma-related interstitial lung disease developed by PSGL-1 deficient mice

Elena González-Sánchez, Antonio Muñoz-Callejas, Javier Gómez-Román, Esther San Antonio, Alessandro Marengo, Nicolas Tsapis, Kamila Bohne-Japiassu, Rafael González-Tajuelo, Saray Pereda, Javier García-Pérez, et al.

Targeted nanotherapy with everolimus reduces inflammation and fibrosis in scleroderma-related interstitial lung disease developed by PSGL-1 deficient mice

Running title: Targeted everolimus therapy for SSc-ILD

Elena González-Sánchez[1], Antonio Muñoz-Callejas[1ϕ], Javier Gómez-Román[2ϕ], Esther San Antonio[1ϕ], Alessandro Marengo[3], Nicolas Tsapis[3], Kamila Bohne-Japiassu[3], Rafael González-Tajuelo[1], Saray Pereda[2], Javier García-Pérez[4], Lorenzo Cavagna[5], Miguel Ángel González-Gay[6], Esther Vicente-Rabaneda[7], Federica Meloni[8], Elias Fattal[3], Santos Castañeda[7,9§] and Ana Urzainqui[1§]

Affiliations:

[1] Immunology Department, Hospital Universitario de la Princesa, Fundación de Investigación Biomédica (FIB), Instituto de Investigación Sanitaria-Princesa (IIS-Princesa), Madrid, Spain.

[2] Pathology Department, Hospital Universitario Marqués de Valdecilla, IDIVAL, Universidad de Cantabria, Santander, Cantabria, Spain.

[3] Institut Galien Paris Sud, UMR CNRS 8612. School of Pharmacy at University Paris-Saclay. Châtenay-Malabry, France.

[4] Pneumology Department, Fundación de Investigación Biomédica (FIB), Instituto de Investigación Sanitaria-Princesa (IIS-Princesa), Hospital Universitario de la Princesa, Madrid, Spain.

[5] Rheumatology Department, University and IRCCS Policlinico S. Matteo Foundation, Università degli Studi di Pavia, Pavia, Italy.

[6] Rheumatology Department, Hospital Universitario Marqués de Valdecilla, IDIVAL, Universidad de Cantabria, Santander, Spain.

[7] Rheumatology Department, Hospital Universitario de la Princesa, Fundación de Investigación Biomédica (FIB), Instituto de Investigación Sanitaria-Princesa (IIS-Princesa), Madrid, Spain.

[8] Internal Medicine Department, Pneumology Division, IRCCS San Matteo Foundation and Università degli Studi di Pavia, Pavia, Italy.

[9] Cathedra UAM-Roche, EPID-Future, Department of Medicine, Universidad Autónoma de Madrid (UAM), Madrid, Spain.

[Φ]These authors have equally contributed to this work

[§]**Corresponding authors:**

Ana Urzainqui, Ph.D.
Immunology Department
Telephone: +34915202307
e-mail: urzainquimayayo@gmail.com

Santos Castañeda, PhD. and M.D.
Rheumatology Department
Telephone: +34915202473
e-mail: scastas@gmail.com

Word count: 5469

What is already known:

- The main SSc-ILD therapeutic strategy, prevention of inflammation, is not effective aginst fibrosis.

-Everolimus has immunosuppressive and anti-proliferative properties, but systemic administration has low efficiency and high toxicity.

What this study adds:

-Everolimus encapsulation in liposomes targeted to CD44-expressing lung cells has anti-apoptotic and anti-inflammatory effects.

-Lip-HA+Ev intratracheal administration reduces fibrosis and inflammation in the SSc-ILD present in aged PSGL-$1^{-/-}$ mice.

Clinical significance:

- Lip-HA nanoparticles are a viable strategy to specifically target inflammatory and fibrogenic lung cells.

- Preclinical evidence of everolimus as an efficient drug to reduce lung fibrosis and inflammation.

Abstract

Background and Purpose

Interstitial lung disease (ILD) is the main cause of mortality in systemic sclerosis (SSc) and current therapies available are of low efficacy or high toxicity. Thus, the identification of innovative less toxic and high efficacy therapeutic approaches to ILD treatment is a crucial point. P-selectin Glycoprotein Ligand-1 (PSGL-1) interaction with P-selectin initiates leukocyte extravasation and the lack of its expression brings to SSc-like syndrome with high incidence of ILD in aged mice.

Experimental Approach

Aged PSGL-$1^{-/-}$ mice were used to assay the therapeutic efficacy of an innovative nanotherapy with everolimus (Ev), included in liposomes decorated with high MW hyaluronic acid (LipHA+Ev) and administrated intratracheally to specifically target CD44-expressing lung cells.

Key Results

PSGL-1$^{-/-}$ mice had increased number of CD45+ and CD45- cells, including alveolar and interstitial macrophages, eosinophils, granulocytes and NK cells, and elevated number of myofibroblasts in broncoalveolar lavage (BAL). CD45+ and CD45- cells expressing proinflammatory and profibrotic cytokines were also increased. PSGL-1$^{-/-}$ mice lung histopathology showed increased immune cell infiltration and apoptosis and exacerbated interstitial and peribronchial fibrosis. Targeted nanotherapy with LipHA+Ev reduced BAL number of myofibroblast, cells producing proinflammatory and profibrotic cytokines, and the degree of lung inflammation at histology. LipHA+Ev treatment also provided an important decrease in severity of peribronchial and interstitial lung fibrosis from moderate to mild injury score.

Conclusions and Implications

Our preclinical study in PSGL-1$^{-/-}$ mice indicates that targeted nanotherapy with LipHA+Ev represents an effective treatment for SSc-ILD, reducing the number of inflammatory and fibrotic cells in BAL and reducing inflammation and fibrosis in lungs.

Non-standard abbreviations list

ILD: Interstitial lung disease

SSc: Systemic sclerosis

PSGL-1: P-selectin glycoprotein ligand-1

ECM: extracellular matrix

HA: Hyaluronic acid

BOS: Bronchiolitis obliterans syndrome

SLE: Systemic lupus erythematosus

BAL: Bronchoalveolar lavage

HMW: High molecular weight

LMW: Low molecular weight

WT: Wild-type

LipHA: Hyaluronic acid decorated liposomes

LipHA+Ev: Hyaluronic acid decorated liposomes containing everolimus

DPPE: 1,2-dipalmitoyl-sn-glycero-3-phosphoethanolamine

HA-DPPE: Hyaluronic acid –phospholipid conjugate

EDC: 1-Ethyl-3-(3-dimethylaminopropyl) carbodiimide

NHS: N-Hydroxysuccinimide

TLC: Thin layer chromatography

1H-NMR: Proton nuclear magnetic resonance

FTIR: Fourier-transform infrared spectroscopy

DPPC: 1,2-dipalmitoyl-sn-glycero-3-phosphocholine

mPEG-DSPE: Distearoyl-sn-glycero-3-phosphoethanolamine-N-[methoxy(polyethylene glycol)-2000] (ammonium salt)

Chol: Cholesterol

RT: Room temperature

PTFE: Polytetrafluoroethylene

PBS: Phosphate buffer saline

BSA: Bovine serum albumin

EDTA: Ethylenediaminetetraacetic acid

FACS: Fluorescence-activated cell sorting

IL: Interleukin

IFN: Interferon

AM: Alveolar macrophages

Eos: Eosinophils

IM: Interstitial macrophages

DC: Dendritic cells

IHQ: Immunohistochemistry

H&E: Hematoxylin and eosin

Keywords: Everolimus / interstitial lung disease / nanotherapy / PSGL-1 / systemic sclerosis.

Introduction

Systemic sclerosis (SSc) is a chronic autoimmune connective tissue disease of unknown origin, characterized by fibrosis, vasculopathy and presence of serum autoantibodies. ILD is the most common organ complication in SSc patients, mainly with diffuse cutaneous SSc, with a prevalence of 53% (Walker *et al.*, 2007) and representing the most frequent cause of mortality in these patients (Steen *et al.*, 2007). SSc-ILD is a severe fibrogenic and inflammatory disorder involving lung interstitium that breaks organ architecture, leading to end stage respiratory failure. Interestingly, increased P-selectin glycoprotein ligand-1 (PSGL-1) expression on dendritic cells have been associated with the presence of ILD in SSc patients (Silvan *et al.*, 2018). Although the etiology, pathogenesis and molecular mechanisms involved in fibrotic activation are not yet completely known, SSc-ILD is histologically characterized by myofibroblast transition and fibroproliferative phase with excess extracellular matrix (ECM) deposition (Silver *et al.*, 2008) and a mixed fibrous-inflammatory pattern (Solomon *et al.*, 2013). Unfortunately, diagnosis is usually made in an advanced fibrotic disease stage and therapeutic intervention, at best, may relent the progression of the disease. The use of immunosuppressive agents is the main therapeutic strategy to prevent the inflammatory phase, but there are few options for its treatment and are not effective against fibrosis (Cottin *et al.*, 2019). Currently, antifibrotic therapies -such as pirfenidone and nintedanib- or biological therapy with tocilizumab or rituximab have been introduced in the therapy of SSc-ILD (Campochiaro *et al.*, 2021). However, these therapies are also associated to a significant degree of systemic toxicity which limits

their application over time (Mirsaeidi *et al.*, 2019). The identification of innovative less toxic therapeutic approaches to this disease is therefore crucial.

Everolimus, a rapamycin derivative, is an mTOR inhibitor endowed with antiproliferative and immunosuppressing properties, initially developed as antineoplastic for specific neoplasms. Besides significant immunoregulatory actions on T and B lymphocytes and other inflammatory effectors, everolimus has demonstrated to suppress fibroblast proliferation *in vitro* (Cova *et al.*, 2015; Chiesa *et al.*, 2018; Pandolfi *et al.*, 2021), therefore it has been adopted with the aim of preventing chronic graft rejection avoiding inflammation and fibrotic progression (Patrucco *et al.*, 2021), but potential side effects and insufficient drug accumulation in target organs, have limited its therapeutic use.

Hyaluronic acid (HA) is a natural extracellular glycosaminoglycan widely distributed throughout tissues as the primary component of the ECM. Its main receptor, CD44, is a ubiquitous and multifunctional surface adhesion receptor having diverse roles in cell–cell and cell–matrix interactions. HA-CD44 interaction plays an important role in physiological and pathological cell regulatory functions (Naor, 2016) and is involved in several disease states such as arthritis, ILD or cancer (Jordan *et al.*, 2015). CD44 is overexpressed in mesenchymal cells and macrophages in lung fibrogenic disorders, including connective tissue disease-associated ILD and bronchiolitis obliterans syndrome (BOS) (Cova *et al.*, 2015; Rios de la Rosa *et al.*, 2017). Recent studies have shown that liposomes functionalised with HA or anti-CD44 antibodies are internalised by lung non-phagocytic cells expressing CD44, like T cells and fibrotic cells (Cova *et al.*, 2015; Cova *et al.*, 2017; Pandolfi *et al.*, 2019). These results make CD44 a useful molecule to develop targeted HA-nanoparticles as drug delivery systems for the treatment of fibrosis (Chiesa *et al.*, 2018; Pandolfi *et al.*, 2019).

PSGL-1, an adhesion molecule expressed on all leukocyte subsets, is the main ligand for P-selectin. The interaction of both molecules under inflammatory conditions activates Syk signalling pathway in leukocytes (Urzainqui *et al.*, 2002) and is involved in their extravasation to inflammation foci (Zarbock *et al.*, 2011). However, the PSGL-1/P-selectin interaction is relevant not only for acute inflammation but also for the maintenance of immune homeostasis (González-Tajuelo *et al.*, 2017; Nunez-Andrade *et al.*, 2011; Urzainqui *et al.*, 2007). The absence of either of these molecules leads to the development of an autoimmune disorder. P-selectin deficiency leads to a systemic lupus erythematosus (SLE)-like syndrome, with altered immunity/tolerance balance, skin alterations and elevated circulating autoantibodies (González-Tajuelo *et al.*, 2017). Likewise, PSGL-1 deficient mice spontaneously develop an autoimmune syndrome similar to human SSc with fibrosis, vascular damage and autoantibodies as well as pulmonary arterial hypertension in female mice (González-Tajuelo *et al.*, 2020; Pérez-Frías *et al.*, 2014). Moreover, 60% of PSGL-$1^{-/-}$ mice older than 12 months develop ILD, with thickening of the pulmonary interstitium, remodelling of lung small vessels medial layer and increased leukocyte infiltrate (Pérez-Frías *et al.*, 2014) in the bronchoalveolar lavage (BAL) and lungs. PSGL-$1^{-/-}$ mice present an imbalance in Th1/Treg populations in the lung, with an increase in the percentage of IFN-γ producing B cells and T cells and a reduction of Treg (González-Tajuelo *et al.*, 2020). The spontaneous and progressive development of ILD with aging in PSGL-$1^{-/-}$ mice, makes this model a very useful tool to search for SSc-ILD treatments, since it is more similar to human pathology than the acute bleomycin model.

Based on these remarks, our goal was to evaluate, in a preclinical study, the therapeutic efficacy of an innovative liposomal formulation of everolimus, locally delivered to the lung of PSGL-$1^{-/-}$ mice with the purpose of developing an effective

inhaled treatment for SSc-ILD patients in the near future. Liposomes have been decorated with high molecular weight hyaluronic acid (HMW-HA) to specifically target CD44, expressed by primary mesenchymal cells and immune cells, and the intratracheal route is studied as an administration strategy to ensure delivery and accumulation of drugs in target cells of all lung segments, thus avoiding most extrapulmonary toxicity.

Materials and Methods

Mice

C57BL/6 PSGL-1$^{-/-}$ mice were kindly provided by Dr. M. K. Wild and Dr. D. Vestweber (Max Planck Institute for Molecular Biomedicine, Münster, Germany). Wild-type (WT) C57BL/6 mice were obtained from The Jackson Laboratory and were backcrossed with PSGL-1$^{-/-}$ mice. Mice were housed in pathogen-free conditions in the Animal Facility of the School of Medicine, Universidad Autónoma de Madrid (Spain), kept at a controlled temperature of 22–25°C with a 12h light–12h darkness cycle and received water and commercial feed ad libitum. Experimental mice were sacrificed by cervical dislocation. All experiments and breeding were performed in accordance with national and institutional guidelines for animal care (EU Directive2010/63/EU for animal experiments). The experimental procedures were approved by the Director General de Medio Ambiente of Madrid (PROEX 104/19). Animal experiments were reported in compliance with the ARRIVE guidelines and with the recommendations made by the British Journal of Pharmacology.

PSGL-1$^{-/-}$ mice develop an autoimmune syndrome similar to human systemic sclerosis and around 60% of animals develop ILD, once they reach 12 months of age, resembling human SSc-ILD. In this work, PSGL-1$^{-/-}$ mice older than 12 months

(ranging from 12 to 20 months and middle age of 16 months) have been used to check whether intratracheal treatment of everolimus encapsulated in liposomes decorated with hyaluronic acid (LipHA-Ev) is able to reduce lung inflammation and fibrosis. In order to have an observable effect of everolimus in the population, and considering that 50% of treated mice might be cured, treatment experiments were designed to have at least 7 mice/group/experiment to find at least 2 cured animals/experiment and hence find a reduction in the number of animals with ILD.

Liposome synthesis, characterization and administration

LipHA+Ev were prepared following the procedure described by Pandolfi et al. (2021) (Pandolfi *et al.*, 2021). First hyaluronic acid–phospholipid conjugate (HA-DPPE conjugate) was synthesized by solubilizing 100mg HA (400KDa) in 20ml of MilliQ® water for 30min. Then, 2M of 1-ethyl-3-(3-dimethylaminopropyl)carbodiimide (EDC) and N-hydroxysuccinimide (NHS) were added and the solution was stirred for more 2h at room temperature (RT). Meanwhile, 5M 1,2-dipalmitoyl-sn-glycero-3-phosphoethanolamine (DPPE) was dissolved in 20ml of tert-butanol/MilliQ® water (9:1 v/v) in the presence of 0.1mol triethylamine and mixed at 55°C and the solution was added drop wise into the HA solution. The resulting mixture was stirred for 6h at 60°C followed by 18h stirring at room temperature. In order to remove free HA, the mixture was dialyzed for 48h against MilliQ® water using 3.5KDa Spectra/Por dialysis bag and then, to completely remove free DPPE, two times centrifugation at 1693xg for 30min was realized. Finally, HA-DPPE solid product was obtained after lyophilization. The synthesis was validated by thin layer chromatography (TLC) using F254 silica gel pre-coated sheets (Sigma-Aldrich) and a mixture of chloroform/methanol 70:30 v/v as mobile phase and visualized using molybdenum blue solution. Proton nuclear magnetic resonance (^{1}H-NMR), nuclear magnetic resonance spectroscopy at 400 MHz (Bruker

Avance III HD 400 spectrometer) and fourier-transform infrared spectroscopy (Perkin Elmer FTIR Spectrum Two) (FTIR) were also performed as additional confirmation.

LipHA+Ev were produced by solvent injection method respecting a 1/10 drug/lipid ratio (w/w). A total amount of 40mg of lipids (26mg 1,2-dipalmitoyl-sn-glycero-3-phosphocholine (DPPC), 6.3mg cholesterol (Chol), 3.7mg Distearoyl-sn-glycero-3-phosphoethanolamine-N-[methoxy(polyethylene glycol)-2000] (ammonium salt) mPEG-DSPE, 4mg HA-DPPE) and 4mg of everolimus were solubilized in 2ml of tert-butanol/water mixture (60:40 v/v) and stirred at 43°C for 10min. Then, the organic solution was injected at a 1.3 ml/min rate into 10ml of MilliQ® water with helps of an automatic injector. The suspension was stirred for 15min at 900 rpm and the solvent was eliminated using a rotary evaporator (RT+20 mbar). To eliminate free HA-DPPE, an ultracentrifugation (72446xg) was performed for 4h at 4°C. Finally, liposomes were centrifuged for 30min at 1693xg in order to eliminate non encapsulated everolimus that precipitated in the pellet. The amount of encapsulated everolimus was evaluated by using a Lambda 25 UV/VIS spectrometer (PerkinElmer). To start, a calibration curve was determined by preparing a solution of 20µg/ml of everolimus in acetonitrile and subsequent dilution in the range of 20µg/ml to 0.5µg/ml. Then, liposomes were diluted by a factor 50 in acetonitrile, vortexed and filtered on 200nm polytetrafluoroethylene (PTFE) filters to remove all the phospholipids. The resulting solution was analyzed in the range of 400 to 200nm and the absorption peak of everolimus was identified at 278nm.

Experimental schedule

PSGL-$1^{-/-}$ and WT mice older than 12 months were randomly distributed into 4 experimental groups of similar size and age animals: WT and PSGL-$1^{-/-}$ control groups without treatment, PSGL-$1^{-/-}$ mice treated with empty liposomes decorated with HMW-

HA (LipHA) and PSGL-1$^{-/-}$ mice treated with LipHA containing everolimus (LipHA+Ev). The age of the animals were matched among the different groups in such a way that the animals of every group had similar age

Treated mice received 4 doses of liposomes (50µL of liposomes/dose) containing 85µg/mL of everolimus or empty LipHA, once a week. Three to five days after the last dose, all animals were sacrificed (Fig 1A). BAL and lungs were obtained and analyzed by flow cytometry or histology in blinded way, respectively. To avoid biased results, three independent experiments (of at least 7 animals/group) were performed for the analysis of BAL cell populations. For histopathology analysis, lungs from 12 animals treated in different experiments were used. Twelve mice were used to check cytokine expression in BAL cells. To check the procedure impact in BAL populations, an experiment was performed by intratracheal insufflation of water to 7 aged PSGL-1$^{-/-}$ animals.

Intratracheal administration

For intratracheal drug administration, we used a handmade insufflator following the video and indications reported by Durham et al. (Durham *et al.*, 2017). To check if the insufflator was working properly and hence the treatment bilaterally reached the alveolar interstitium, a contrast agent (Iopamiro 300®) was intratracheally introduced and visualized by X-ray (supplementary Fig 1).

Before treatment, mice were anesthetised subcutaneously with 150µL of a mixture of: Medetomidine hydrochloride 0.05mg/mL, Ketamine 2mg/mL, Midazolam 0.5mg/mL and Butorphanol 0.2mg/mL. To reverse anaesthesia after intratracheal treatment, 150µL of a solution containing Flumazenil 25µg/mL and Antipamezole 0.25mg/mL were subcutaneously administered to animals.

BAL and lungs obtention and processing

For BAL collection, the trachea was perforated between the first two tracheal rings and a 21G Abbocath catheter was introduced through the hole and fixed with surgical suture, by knotting the surgical suture around the trachea. One mL of PBS was infused into the lungs and aspirated twice and the BAL cell suspension was kept in cold until use. Then, cells were centrifuged and resuspended in PBS 1x BSA 0.5% EDTA 5mM and labelled for flow cytometry.

For histological analysis, lungs were dissected, fixed in 4% paraformaldehyde for 48 hours, and dehydrated. Lungs were embedded in paraffin and cut into 3µm slices.

Flow Cytometry

Briefly, individual BAL cells were incubated with 1:600 Fc Block (BD Pharmingen). After incubation, cells were stained with a cocktail of surface antibodies for 30min at 4°C. After washing, cells were fixed and permeabilized with 2ml of FACS Lysing Solution (BD Pharmingen) for 15 minutes. Then, cells were washed and incubated with an intracellular antibody cocktail for 30 minutes at 4°C. Five µL of CountBright absolute counting beads (Invitrogen) were added to each tube for the assessment of the absolute number of cells present in the BAL. Finally, samples were acquired and analysed with a FACS Canto II and FACS Diva software.

Cell gating strategy and flow cytometry reagents

Different antibody panels were designed for the identification of BAL immune cell populations using monoclonal antibodies summarised in supplementary Table I.

Immune cells were identified by a prior discrimination of cell fractions based on size-complexity assessment by forward scatter/side scatter parameters and by gating as

CD45+ cells. The expression of IFN-γ, IL-10, IL-6 and IL-17 cytokines, and the CD44 receptor was analysed in both CD45+ and CD45- subsets. Myofibroblast were identified as CD44+α-SMA+ in the total BAL cells. For characterisation of myeloid BAL cells, alveolar macrophages (AM) and eosinophils (Eos) were gated as SiglecF+CD11c+ and SiglecF+CD11c-, respectively. Interstitial macrophages (IM) were gated as SiglecF-CD11c-CD11b+ and dendritic cells (DC) were gated as SiglecF-CD11c+ (Fig 2A). Neutrophils (Neut, Gr1) were gated as Ly6G+Ly6C+. Lymphoid BAL cell populations were gated as follows: B cells (Gr1-CD19+), T cells (Gr1-CD3+) and NK (Gr1-CD19-CD3-CD49b+) (Fig 3A).

For identification of CD45-CD44+ populations, lung and BAL cells were labelled with CD45, CD44, CD31, CD90.2 and EpCAM. First, CD44+ cells were gated and then, CD45+ and CD45- were identified in the CD44+ cells. Endothelial cells were identified as CD45-CD31+, epithelial cells were identified as CD45-EpCAM+ cells and fibroblasts were identified as CD45-CD90.2+ cells (Fig 1). Apoptotic cells were analyzed in each population by the expression of annexin V.

Lung pathology analysis

Lung sections were stained with hematoxylin and eosin (H&E) and Masson's trichrome to assess inflammatory infiltration and fibrotic extension, respectively. Stainings were independently analysed by a pathologist blinded to the study. The degree of interstitial inflammation as well as peribronchial and interstitial fibrosis were evaluated and assigned to a lung injury score using a numerical scale from 0 to 3 (0: absence; 1: mild, 2: moderate, 3: severe).

Lung immunohistochemistry

Immunohistochemistry staining was performed in paraffin-embedded lung sections, conforms to BJP Guidelines. Lung murine leukocytes were identified as CD45+ cells by staining for CD45 (with mouse monoclonal antibody FLEX CD45 LCA, MxH [2B11+PD7/26] from Dako/Agilent. Lung cell apoptosis was assessed by Caspase 3 staining of lung sections (Clone C92-605 purified rabbit anti-active caspase 3, BD Biosciences). For Collagen I staining Abcam 6308 anti-collagen I antibody was used. Stainings were carried out following the manufacture's instruction for each antibody. To analyse the presence of apoptotic cells in untreated versus treated animals, lung sections from 5 PSGL-$1^{-/-}$ mice, 5 LipHA treated and 5 LipHA+Ev treated PSGL-$1^{-/-}$ animals were stained with caspase 3 by immunohistochemical assay (IHQ). As basal control of caspase 3 staining in aged WT animals, lung sections from 2 WT aged animals were stained by IHQ with caspase 3. For caspase 3+ quantification, staining of Caspase 3 was checked in the whole histological section to identify aggregates of caspase 3+ cells and the number of positive cells in the larger aggregates were counted. Data indicate the maximum number of positive cells in a 40x objective field (0, 2 mm^2).

Data and analysis

The manuscript complies with BJP´s recommendations and requirements on experimental design and analysis. In all experiments, the declared group size is the number of independent values obtained from different mice and statistical analysis was done using these independent values.

In all cases, data are the direct values obtained, without any transformation, no approaches for data normalization nor to generate normal data were applied. In all cases, the important point was to analyze differences between untreated PSGL-$1^{-/-}$ and

LipHA+Ev treated mice. Also, as control of the presence of ILD in the absence of PSGL-1, WT and PSGL-$1^{-/-}$ mice were checked. In addition, we checked whether LipHA had any effect in the fibrosis an inflammation with respect to untreated mice as well as with respect to LipHA+Ev treated mice. For this purpose, the corresponding comparisons between two groups were performed. Normality of the variables was tested using the Shapiro-Wilk test. For nonparametric variables, statistical differences between groups were evaluated using Mann-Whitney U test. All values are shown as mean ± standard error of the mean (SEM). All statistical analyses were performed using GraphPad Prism 6 (GraphPad Software). In all cases p values <0.05 were considered as statistically significant. Statistical analysis for quantitative data was undertaken for groups with at least n=5. Only experiments done for qualitative analysis (immunohistochemistry and Masson´s trichrome staining) were included without statistical analysis. Outliers were excluded.

Results

CD44 expression in lung and BAL cells of aged PSGL-$1^{-/-}$ mice

The expression of CD44 was analysed in lung and BAL cells obtained from aged WT and PSGL-$1^{-/-}$ mice. We found increased numbers of CD44+ cells in lungs and BAL of PSGL-$1^{-/-}$ mice compared to WT animals (Fig 1B and F). Interestingly, in PSGL-$1^{-/-}$ lungs the CD45+ subset was increased in the CD44+ population while the number of CD45- cells was similar to that of WT animals (Fig 1B). Also, the expression level of CD44 in the CD45+ subset showed a tendency to be higher in PSGL-$1^{-/-}$ than WT mice (Fig 1C). Deeper analysis of the CD45- subpopulation was addressed in lung and BAL of WT and PSGL-$1^{-/-}$ mice (CD90.2+ fibroblasts, EpCAM+ epithelial cells

and CD31+ endothelial cells) (Fig 1D and H). In lungs, we did not find differences between WT and KO mice in the number of epithelial cells, endothelial cells and fibroblasts present in the CD44+ population (Fig 1D) or in the expression level of CD44 in these subpopulations (Fig 1E).

In the BAL of PSGL-1$^{-/-}$ mice both, the CD45+ and CD45- subsets were increased in the CD44+ population (Fig 1F), although the expression level of CD44 was similar to WT mice in both subsets (Fig 1G). Regarding the CD45- subpopulations, the number of fibroblasts was increased in the CD44+ population of PSGL1$^{-/-}$ mice, no endothelial cells were detected in WT or KO mice and the number of epithelial cells in the CD44+ population was similar in PSGL-1$^{-/-}$ and WT mice (Fig 1H). The CD44 expression level in epithelial cells and fibroblasts was similar in WT and PSGL-1-/- mice (Fig 1I).

Treatment with LipHA+Everolimus reduces the presence of immune and CD45- cell populations in the BAL of PSGL-1$^{-/-}$ mice

The impact of the procedure on BAL populations was checked by intratracheal introduction of water. Data showed no changes, except for an increment of interstitial macrophages (Suppl. Fig 2)

The analysis by flow cytometry (Fig 2A) of cell populations present in the BAL of untreated or treated mice showed that untreated aged PSGL-1$^{-/-}$ mice presented increased total number of CD45+ cells compared to WT mice (Fig 2B). Treatment with LipHA+Ev reduced this difference, although this reduction was not statistically significant (Fig 2B). Detailed analysis of the different BAL immune cell populations showed that untreated PSGL-1$^{-/-}$ animals had higher absolute numbers of alveolar macrophages (AM), interstitial macrophages (IM), eosinophils (Eos), granulocytes

(Gr1), NK cells and a tendency to increased number of dendritic cells (DC) and T lymphocytes that were not statistically significant (Figs 2C-F and Figs 3B-D). No differences in B cells were observed between groups. Regarding CD45- cells, untreated PSGL-1$^{-/-}$ mice also presented a significant expansion of CD45- cells in the BAL (Fig 2G). Interestingly, intratracheal treatment with LipHA+Ev reduced to WT levels the number of AM and CD45- cells in PSGL-1$^{-/-}$ mice (Figs 2C, G). The number of IM and Eos was also reduced, losing the differences with the WT mice (Figs 2E, F). Treatment with empty liposomes reduced the number of AM (Fig 2C). Moreover, empty LipHA administration increased the number of Gr1, T cells and NK cells in the BAL but everolimus prevented this increase, remaining at the levels of untreated PSGL-1$^{-/-}$ mice (Figs 3B-D).

Histopathological effects of LipHA+Everolimus treatment in PSGL-1$^{-/-}$ mice

To check the effect of everolimus in the lung structure of treated mice, we evaluated immune cell infiltration (Fig 4A) as well as interstitial and peribronchial fibrosis in the lungs after treatment with LipHA+Ev (Figs 5A, B). Lung histopathology showed an enhanced interstitial inflammation in PSGL-1$^{-/-}$ animals compared to WT mice (mean lung injury score ± SEM: 1.58±0.31 vs 0.2±0.13). While 80% of WT mice had absence of lung injury and 20% showed mild injury, in the PSGL-1$^{-/-}$ group only 25% showed no injury while 17% had severe disease and 50% had moderate injury. On average, PSGL-1$^{-/-}$ animals had a moderate lung injury score that was maintained in LipHA treated animals (1.17±0.24). However, LipHA+Ev administration reduced the severity of this interstitial inflammation from moderate to mild levels (0.92±0.31), with up to 41% of the analysed animals showing mild interstitial inflammation and 42% of the analysed animals without interstitial inflammatory disease (Figs 4A, B). CD45 immunohistochemical staining of lung sections confirmed these data (Fig 4C).

Regarding fibrosis, the histopathological analysis showed that interstitial and peribronchial lung fibrosis were increased in PSGL-$1^{-/-}$ mice compared to WT animals (1.08±0.34 vs 0.4±0.16 and 1±0.33 vs 0.2±0.13, respectively). PSGL-$1^{-/-}$ mice treated with empty LipHA maintained moderate interstitial and peribronchial fibrosis (1±0.25 and 1.5±0.31 respectively), while LipHA+Ev treatment reduced the severity of both type of fibrosis to a mild score (0.67±0.28 and 0.58±0.26, respectively) (Figs 5A, B), demonstrating a significant capacity of everolimus to reduce fibrogenic lung lesions. Remarkably, everolimus increased the percentage of animals without interstitial and without peribronchial fibrosis and reduced the number of animals with severe fibrosis. These data were confirmed by Masson's trichrome staining (Fig 5C) and IHQ with anti-collagen I antibodies of lung sections (Fig 5D).

Cytokine expression in BAL cells after treatment with LipHA+Everolimus

To understand the mechanism responsible of the reduction of lung disease observed in PSGL-$1^{-/-}$ mice after treatment with LipHA+Ev, we assessed functional difference in CD45+ and CD45- BAL cells of control and treated mice, by analysing the expression of proinflammatory (IFN-γ, IL-17 and IL-6) and profibrotic (IL-10, IL-17, IL-6) cytokines (Figs 6A-E). IFN-γ, IL-10 and IL-6 were determined in CD45+ BAL cells and IL-17 and IL-6 expression were measured in CD45- cells. PSGL-$1^{-/-}$ control mice exhibited an increase in IL-6, IL-10 and IL-17 cytokines compared with WT animals. Treatment with both, LipHA and LipHA+Ev reduced the number of CD45+ cells expressing IFN-γ (Fig 6A), IL-6 (Fig 6B) and IL-10 (Fig 6C, left panel) cytokines. Although LipHA and LipHA+Ev had the same effect in reducing the number of cells expressing IFN-γ and IL-6 (Figs 6A-B), LipHA+Ev had a stronger effect in reducing the presence of IL-10+CD45+ cells (Fig 6C, right panel).

Regarding BAL CD45- cells, PSGL-1$^{-/-}$ mice cells showed higher number of cells expressing IL-6 and IL-17 and treatment with LipHA+Ev reduced both subpopulations (Figs 6D, E), losing the difference with WT animals. This effect was also observed with LipHA.

LipHA+Everolimus treatment reduces the presence of myofibroblasts in BAL and apoptotic cells in lungs

Since treatment with LipHA+Ev reduced CD45+ and CD45- BAL cells and lung fibrosis, we further investigated its effect on myofibroblasts presence in BAL. PSGL-1$^{-/-}$ mice showed highly increased number of myofibroblast and LipHA+Ev treatment reduced this population to numbers found in WT mice (Fig 7A, left panel). We also studied the presence of apoptosis in the lungs of untreated and LipHA+Ev treated mice by Caspase 3 staining. PSGL-1$^{-/-}$ mice exhibited increased caspase 3+ cells compared to WT animals. LipHA+Ev treatment reduced the presence of apoptotic cells, while the treatment with LipHA was unable to reduce it (Figs 7B, C). To check the cell subsets suffering apoptosis, a deeper analysis was performed by studying the expression of annexin V in different lung cell subsets. We have found that both, CD45+ and CD45- lung subsets of PSGL-1$^{-/-}$ mice had increased number of annexin V+ cells than that of WT mice (Fig. 7D). Interestingly, epithelial cells, endothelial cells and fibroblasts of PSGL-1$^{-/-}$ presented higher number of apoptotic cells than that of WT mice (Fig. 7E)

Discussion

In this work, we have studied the curative effect of everolimus on the process of ILD evolution related to inflammation and aging of PSGL-1$^{-/-}$ mice. Since orally administration of everolimus has been shown to induce a more rapid disease

progression in idiopathic pulmonary fibrosis (IPF) patients (Malouf *et al.*, 2011), we have encapsulated everolimus into liposomes targeting CD44 expressing cells to avoid drug toxicity. For this purpose, liposomes were coated with HMW-HA to take advantage of its higher CD44 receptor affinity and the anti-inflammatory action reported with respect to low molecular weight (LMW)-HA (Litwiniuk *et al.*, 2016; Pandolfi *et al.*, 2021). In addition, *in vitro* experiments have shown higher everolimus effect when is included in LipHA than the drug alone (Chiesa *et al.*, 2018; Pandolfi *et al.*, 2021). To limit systemic toxicity, liposomes were administered intratracheally. We have found that this treatment strategy efficiently reduced both, lung inflammation and fibrosis. Remarkably, this work is a preclinical study in a mouse model with established SSc-ILD at the time of initiation of treatment.

Development of preclinical animal models that recapitulate human diseases is an essential tool to test new treatment strategies to find the appropriate treatment for diseases. PSGL-$1^{-/-}$ mouse model presents the main clinical characteristics of human scleroderma, including SSc-ILD (González-Tajuelo *et al.*, 2020; Pérez-Frías *et al.*, 2014), the most common organ complication in SSc and the most frequent cause of mortality in these patients (Steen *et al.*, 2007). In this work, the lung histopathological study showed that 75% of aged PSGL-$1^{-/-}$ mice had lung inflammation and 60% had interstitial fibrosis and, accordingly, CD45- and CD45+ cell populations were also increased in the BAL of these mice, including AM, IM, granulocytes, eosinophils and NK cells, as also described for patients with ILD (Meyer *et al.*, 2012; Solomon *et al.*, 2013).

Importantly, in PSGL-$1^{-/-}$ mice BAL we found higher number of CD45+ cells expressing IFN-γ, IL-10 and IL-6, as well as elevated number of CD45- cells expressing IL-6 and IL-17. Likewise, high levels of cytokines have been reported for SSc-ILD

patients in BAL, serum and affected tissues (Meloni *et al.*, 2004; Sato *et al.*, 2001). Of note, treatment with LipHA+Ev reduced the presence of immune cells and CD45- population in the BAL, as well as populations expressing these proinflammatory and profibrotic cytokines. These results are in accordance to previous *in vitro* results showing that everolimus reduces IFN-γ and IL-10 production (Cova *et al.*, 2017; Pandolfi *et al.*, 2021). The reduced expression of these cytokines may explain the improvement of lung histopathology observed after treatment. We have found that everolimus has a specific effect on the reduction of cells producing IL-10. Markedly, IL-10 is a well-known anti-inflammatory cytokine with pro-fibrogenic properties (Sziksz *et al.*, 2015). Thus, we can hypothesize that, at least in part, LipHA+Ev efficacy in our model might be mediated by the modulation of IL-10 lung production.

Our data indicates that also "empty LipHA" have a direct modulatory effect on the inflammation of lung microenvironment. The liposomes induced an increased frequency of eosinophils, granulocytes, T cells and NK cells in the BAL, which was previously reported for CD44 (Baaten *et al.*, 2012; Galandrini *et al.*, 1996; Ohkawara *et al.*, 2000; Pandolfi *et al.*, 2019). Remarkably, everolimus was clearly able to counteract the increment of inflammatory cells in lungs promoted by LipHA. Otherwise, LipHA were able to reduce the frequency of cells expressing IFN-γ, IL-6 and IL-17, and this might be partly due to the anti-inflammatory properties of HMW-HA (Rooney et al., 2015), cooperating with Ev in the anti-inflammatory effect in SSc-ILD.

PSGL-1$^{-/-}$ mice presented an increased myofibroblast population in BAL, as reported for SSc-ILD patients (Silver *et al.*, 2008). CD44-HA signalling could be involved in the increased peribronchial fibrosis severity observed in mice treated with empty LipHA, since this interaction has been described to induce myofibroblast differentiation and activation (Midgley *et al.*, 2013). Remarkably, our work shows that

LipHA+Ev reduces both peribronchial and interstitial lung fibrosis as well as the number of myofibroblasts in the BAL of treated mice, pointing to the antifibrotic effect of everolimus in the efficacy of LipHA+Ev treatment. Therefore, everolimus encapsulation into nanoparticles seems to be a viable strategy to specifically target fibrotic cells in the lung and to reduce their proliferation, as reported *in vitro* (Cova *et al.*, 2015; Chiesa *et al.*, 2018).

Moreover, we have found that the presence of caspase3+ cells is highly increased in the lungs of PSGL-$1^{-/-}$ mice and that LipHA+Ev treatment reduces the presence of caspase3+ cells in the lungs. Apoptosis has been associated with SSc pathogenesis, since accumulation of apoptotic cells in tissues may contribute to tissue damage and fibrosis (Barnes *et al.*, 2011). Our data suggest that everolimus may affect lung damage and fibrosis by promoting an antiapoptotic effect in lung cells of PSGL-$1^{-/-}$ mice that reduces the presence of caspase3+ cells. A similar effect was found in a hepatic mouse model of ischemia-reperfusion injury after liver transplantation (Barnes *et al.*, 2011; Lee *et al.*, 2016).

Nanotechnology opens a new way for SSc-ILD treatment, avoiding secondary lung toxicity by specifically targeting drugs to pathogenic cells (Cova *et al.*, 2017; Lee *et al.*, 2016). The choice of an adequate nanovector is crucial since it can accumulate in lung tissue as has been observed with gold nanoparticles (Codullo *et al.*, 2019; Cova *et al.*, 2017). In this regard we used liposomes, which are highly biodegradable nanoparticles suitable for a long-term therapy, whose biocompatibility has already been tested (Nascimento *et al.*, 2015; Pandolfi *et al.*, 2019). Another crucial point is to reduce drug toxicity. In this study we have loaded everolimus into liposomes previously decorated with HMW-HA to target drug delivery to cells expressing its main ligand, CD44. CD44 is a membrane glycoprotein involved in different cellular functions, whose

expression is up-regulated in autoimmune diseases, including SSc (Cova *et al.*, 2015; Ghatak *et al.*, 2017). Likewise, we have found that PSGL-1$^{-/-}$ mice present increased number of cells expressing CD44. Accordingly, LipHA target everolimus delivery to CD44 expressing cells, avoiding systemic distribution and tissue damage. Moreover, LipHA concentrate everolimus in the target cells, thus improving its inhibitory effect. In addition, the intratracheal administration ensures the delivery of liposomes to the damaged tissue. Using this delivery route, we have been able to reduce the established fibrosis and inflammation in the lungs of aged PSGL-1$^{-/-}$ mice. This result is very promising for SSc-ILD patients, who are generally diagnosed when lung fibrosis is established and its resolution is critical to the life of patients.

At the moment, the therapeutic options for SSc-ILD treatment are scarce, poorly effective and their use is restricted in time due to their high toxicity (Mirsaeidi *et al.*, 2019). Therefore, new safe and efficient treatment strategies are urgently needed. In this preclinical study for SSc-ILD treatment, we have found that drug encapsulation into Lip-HA nanoparticles seems to be a viable strategy to specifically target fibrotic lung cells and that everolimus is an efficient drug to reduce fibrosis and inflammation.

Authors Statement

Authors have followed the recommendations set out in the BJP editorials where they are relevant.

Acknowledgments

We thank the UAM animal facility for animal breeding and care. We also thank the Cytometry Unit and Statistical and Methodological Support Unit of the Hospital de la Princesa for technical support. We thank Manuel Gómez for manuscript editing. We also thank Danae Díaz-Caneja and Vicente González, from the Clínica Veterinaria Exóticos, Fuenlabrada, Madrid (Spain), for participating in the set-up of the experiments.

This work was supported by European Innovative Research & Technological Development (ARROW-NANO Project, EURONANOMED AC 2017/00027) and by Spanish Ministry of Health and Instituto de Salud Carlos III (ISCIII) (cofinanced by European Regional Development Fund, Fondos FEDER) [grant numbers: AC17-00027, FIS-PI17-01819 and FIS-PI20-01690].

Author contributions

AU and SC conceived, supervised the study and provided the necessary funding to carry out the project. EG-S and AU designed and interpreted the experiments and analysed data. EG-S performed most of the experiments and wrote the manuscript. AM-C, ESA and RGT performed mice experiments. JG-R, SP and MAG-G performed histopathological lung studies. AM, NT, KB-J and EF synthesised liposomes. EV-R, JG-P, LC, FM and SC gave clinical advice. All the authors contributed to discuss the data and revised the manuscript.

Conflict of Interest:

The authors declare no competing financial interests.

Declaration of transparency and scientific rigour

This Declaration acknowledges that this study adheres to the principles for transparent reporting and scientific rigour of preclinical research as stated in the BJP guidelines for Design & Analysis, and Animal Experimentation.

References

Baaten, BJ, Tinoco, R, Chen, AT, Bradley, LM (2012) Regulation of Antigen-Experienced T Cells: Lessons from the Quintessential Memory Marker CD44. *Front Immunol* **3:** 23.

Barnes, TC, Spiller, DG, Anderson, ME, Edwards, SW, Moots, RJ (2011) Endothelial activation and apoptosis mediated by neutrophil-dependent interleukin 6 trans-signalling: a novel target for systemic sclerosis? *Ann Rheum Dis* **70**(2)**:** 366-372.

Campochiaro, C, Allanore, Y (2021) An update on targeted therapies in systemic sclerosis based on a systematic review from the last 3 years. *Arthritis Res Ther* **23**(1)**:** 155.

Codullo, V, Cova, E, Pandolfi, L, Breda, S, Morosini, M, Frangipane, V, Malatesta, M, Calderan, L, Cagnone, M, Pacini, C, Cavagna, L, Recalde, H, Distler, JHW, Giustra, M, Prosperi, D, Colombo, M, Meloni, F, Montecucco, C (2019) Imatinib-loaded gold nanoparticles inhibit proliferation of fibroblasts and macrophages from systemic sclerosis patients and ameliorate experimental bleomycin-induced lung fibrosis. *J Control Release* **310:** 198-208.

Cottin, V, Brown, KK (2019) Interstitial lung disease associated with systemic sclerosis (SSc-ILD). *Respir Res* **20**(1)**:** 13.

Cova, E, Colombo, M, Inghilleri, S, Morosini, M, Miserere, S, Penaranda-Avila, J, Santini, B, Piloni, D, Magni, S, Gramatica, F, Prosperi, D, Meloni, F (2015) Antibody-engineered nanoparticles selectively inhibit mesenchymal cells isolated from patients with chronic lung allograft dysfunction. *Nanomedicine (Lond)* **10**(1)**:** 9-23.

Cova, E, Inghilleri, S, Pandolfi, L, Morosini, M, Magni, S, Colombo, M, Piloni, D, Finetti, C, Ceccarelli, G, Benedetti, L, Cusella, MG, Agozzino, M, Corsi, F, Allevi, R, Mrakic-Sposta, S, Moretti, S, De Gregori, S, Prosperi, D, Meloni, F (2017) Bioengineered gold nanoparticles targeted to mesenchymal cells from patients with bronchiolitis obliterans syndrome does not rise the inflammatory response and can be safely inhaled by rodents. *Nanotoxicology* **11**(4)**:** 534-545.

Chiesa, E, Dorati, R, Conti, B, Modena, T, Cova, E, Meloni, F, Genta, I (2018) Hyaluronic Acid-Decorated Chitosan Nanoparticles for CD44-Targeted Delivery of Everolimus. *Int J Mol Sci* **19**(8).

Durham, PG, Hanif, SN, Contreras, LG, Young, EF, Braunstein, MS, Hickey, AJ (2017) Disposable Dosators for Pulmonary Insufflation of Therapeutic Agents to Small Animals. *J Vis Exp*(121).

Galandrini, R, Piccoli, M, Frati, L, Santoni, A (1996) Tyrosine kinase-dependent activation of human NK cell functions upon triggering through CD44 receptor. *Eur J Immunol* **26**(12)**:** 2807-2811.

Ghatak, S, Markwald, RR, Hascall, VC, Dowling, W, Lottes, RG, Baatz, JE, Beeson, G, Beeson, CC, Perrella, MA, Thannickal, VJ, Misra, S (2017) Transforming growth factor beta1 (TGFbeta1) regulates CD44V6 expression and activity through extracellular signal-regulated kinase (ERK)-induced EGR1 in pulmonary fibrogenic fibroblasts. *J Biol Chem* **292**(25)**:** 10465-10489.

González-Tajuelo, R, de la Fuente-Fernandez, M, Morales-Cano, D, Munoz-Callejas, A, González-Sánchez, E, Silvan, J, Serrador, JM, Cadenas, S, Barreira, B, Espartero-Santos, M, Gamallo, C, Vicente-Rabaneda, EF, Castaneda, S, Perez-Vizcaino, F, Cogolludo, A, Jimenez-Borreguero, LJ, Urzainqui, A (2020) Spontaneous Pulmonary Hypertension Associated With Systemic Sclerosis in P-Selectin Glycoprotein Ligand 1-Deficient Mice. *Arthritis Rheumatol* **72**(3)**:** 477-487.

González-Tajuelo, R, Silvan, J, Perez-Frias, A, de la Fuente-Fernandez, M, Tejedor, R, Espartero-Santos, M, Vicente-Rabaneda, E, Juarranz, A, Munoz-Calleja, C, Castaneda, S, Gamallo, C, Urzainqui, A (2017) P-Selectin preserves immune tolerance in mice and is reduced in human cutaneous lupus. *Sci Rep* **7:** 41841.

Jordan, AR, Racine, RR, Hennig, MJ, Lokeshwar, VB (2015) The Role of CD44 in Disease Pathophysiology and Targeted Treatment. *Front Immunol* **6:** 182.

Lee, SC, Kim, KH, Kim, OH, Lee, SK, Kim, SJ (2016) Activation of Autophagy by Everolimus Confers Hepatoprotection Against Ischemia-Reperfusion Injury. *Am J Transplant* **16**(7)**:** 2042-2054.

Litwiniuk, M, Krejner, A, Speyrer, MS, Gauto, AR, Grzela, T (2016) Hyaluronic Acid in Inflammation and Tissue Regeneration. *Wounds* **28**(3)**:** 78-88.

Malouf, MA, Hopkins, P, Snell, G, Glanville, AR (2011) An investigator-driven study of everolimus in surgical lung biopsy confirmed idiopathic pulmonary fibrosis. *Respirology* **16**(5)**:** 776-783.

Meloni, F, Caporali, R, Marone Bianco, A, Paschetto, E, Morosini, M, Fietta, AM, Bobbio-Pallavicini, F, Pozzi, E, Montecucco, C (2004) Cytokine profile of bronchoalveolar lavage in systemic sclerosis with interstitial lung disease: comparison with usual interstitial pneumonia. *Ann Rheum Dis* **63**(7)**:** 892-894.

Meyer, KC, Raghu, G, Baughman, RP, Brown, KK, Costabel, U, du Bois, RM, Drent, M, Haslam, PL, Kim, DS, Nagai, S, Rottoli, P, Saltini, C, Selman, M, Strange, C, Wood, B (2012) An official American Thoracic Society clinical practice guideline: the clinical utility of bronchoalveolar lavage cellular analysis in interstitial lung disease. *Am J Respir Crit Care Med* **185**(9)**:** 1004-1014.

Midgley, AC, Rogers, M, Hallett, MB, Clayton, A, Bowen, T, Phillips, AO, Steadman, R (2013) Transforming growth factor-beta1 (TGF-beta1)-stimulated fibroblast to myofibroblast differentiation is mediated by hyaluronan (HA)-facilitated epidermal growth factor receptor (EGFR) and CD44 co-localization in lipid rafts. *J Biol Chem* **288**(21)**:** 14824-14838.

Mirsaeidi, M, Barletta, P, Glassberg, MK (2019) Systemic Sclerosis Associated Interstitial Lung Disease: New Directions in Disease Management. *Front Med (Lausanne)* **6:** 248.

Naor, D (2016) Editorial: Interaction Between Hyaluronic Acid and Its Receptors (CD44, RHAMM) Regulates the Activity of Inflammation and Cancer. *Front Immunol* **7:** 39.

Nascimento, TL, Hillaireau, H, Noiray, M, Bourgaux, C, Arpicco, S, Pehau-Arnaudet, G, Taverna, M, Cosco, D, Tsapis, N, Fattal, E (2015) Supramolecular Organization and siRNA Binding of Hyaluronic Acid-Coated Lipoplexes for Targeted Delivery to the CD44 Receptor. *Langmuir* **31**(41)**:** 11186-11194.

Nunez-Andrade, N, Lamana, A, Sancho, D, Gisbert, JP, Gonzalez-Amaro, R, Sanchez-Madrid, F, Urzainqui, A (2011) P-selectin glycoprotein ligand-1 modulates immune inflammatory responses in the enteric lamina propria. *J Pathol* **224**(2)**:** 212-221.

Ohkawara, Y, Tamura, G, Iwasaki, T, Tanaka, A, Kikuchi, T, Shirato, K (2000) Activation and transforming growth factor-beta production in eosinophils by hyaluronan. *Am J Respir Cell Mol Biol* **23**(4)**:** 444-451.

Pandolfi, L, Frangipane, V, Bocca, C, Marengo, A, Tarro Genta, E, Bozzini, S, Morosini, M, D'Amato, M, Vitulo, S, Monti, M, Comolli, G, Scupoli, MT, Fattal, E, Arpicco, S, Meloni, F (2019) Hyaluronic Acid-Decorated Liposomes as Innovative Targeted Delivery System for Lung Fibrotic Cells. *Molecules* **24**(18).

Pandolfi, L, Marengo, A, Japiassu, KB, Frangipane, V, Tsapis, N, Bincoletto, V, Codullo, V, Bozzini, S, Morosini, M, Lettieri, S, Vertui, V, Piloni, D, Arpicco, S, Fattal, E, Meloni, F (2021) Liposomes Loaded with Everolimus and Coated with Hyaluronic Acid: A Promising Approach for Lung Fibrosis. *Int J Mol Sci* **22**(14).

Patrucco, F, Allara, E, Boffini, M, Rinaldi, M, Costa, C, Albera, C, Solidoro, P (2021) Twelve-month effects of everolimus on renal and lung function in lung transplantation: differences in chronic lung allograft dysfunction phenotypes. *Ther Adv Chronic Dis* **12:** 2040622321993441.

Pérez-Frías, A, Gonzalez-Tajuelo, R, Nunez-Andrade, N, Tejedor, R, Garcia-Blanco, MJ, Vicente-Rabaneda, E, Castaneda, S, Gamallo, C, Silvan, J, Esteban-Villafruela, A, Cubero-Rueda, L, Garcia-Garcia, C, Munoz-Calleja, C, Garcia-Diez, A, Urzainqui, A (2014) Development of an autoimmune syndrome affecting the skin and internal organs in P-selectin glycoprotein ligand 1 leukocyte receptor-deficient mice. *Arthritis Rheumatol* **66**(11)**:** 3178-3189.

Rios de la Rosa, JM, Tirella, A, Gennari, A, Stratford, IJ, Tirelli, N (2017) The CD44-Mediated Uptake of Hyaluronic Acid-Based Carriers in Macrophages. *Adv Healthc Mater* **6**(4).

Rooney, P, Srivastava, A, Watson, L, Quinlan, LR, Pandit, A (2015) Hyaluronic acid decreases IL-6 and IL-8 secretion and permeability in an inflammatory model of interstitial cystitis. *Acta Biomater* **19:** 66-75.

Sato, S, Hasegawa, M, Takehara, K (2001) Serum levels of interleukin-6 and interleukin-10 correlate with total skin thickness score in patients with systemic sclerosis. *J Dermatol Sci* **27**(2)**:** 140-146.

Silvan, J, Gonzalez-Tajuelo, R, Vicente-Rabaneda, E, Perez-Frias, A, Espartero-Santos, M, Munoz-Callejas, A, Garcia-Lorenzo, E, Gamallo, C, Castaneda, S, Urzainqui, A (2018)

Deregulated PSGL-1 Expression in B Cells and Dendritic Cells May Be Implicated in Human Systemic Sclerosis Development. *J Invest Dermatol* **138**(10)**:** 2123-2132.

Silver, RM, Wells, AU (2008) Histopathology and bronchoalveolar lavage. *Rheumatology (Oxford)* **47 Suppl 5:** v62-64.

Solomon, JJ, Olson, AL, Fischer, A, Bull, T, Brown, KK, Raghu, G (2013) Scleroderma lung disease. *Eur Respir Rev* **22**(127)**:** 6-19.

Steen, VD, Medsger, TA (2007) Changes in causes of death in systemic sclerosis, 1972-2002. *Ann Rheum Dis* **66**(7)**:** 940-944.

Sziksz, E, Pap, D, Lippai, R, Beres, NJ, Fekete, A, Szabo, AJ, Vannay, A (2015) Fibrosis Related Inflammatory Mediators: Role of the IL-10 Cytokine Family. *Mediators Inflamm* **2015:** 764641.

Urzainqui, A, Martinez del Hoyo, G, Lamana, A, de la Fuente, H, Barreiro, O, Olazabal, IM, Martin, P, Wild, MK, Vestweber, D, Gonzalez-Amaro, R, Sanchez-Madrid, F (2007) Functional role of P-selectin glycoprotein ligand 1/P-selectin interaction in the generation of tolerogenic dendritic cells. *J Immunol* **179**(11)**:** 7457-7465.

Urzainqui, A, Serrador, JM, Viedma, F, Yanez-Mo, M, Rodriguez, A, Corbi, AL, Alonso-Lebrero, JL, Luque, A, Deckert, M, Vazquez, J, Sanchez-Madrid, F (2002) ITAM-based interaction of ERM proteins with Syk mediates signaling by the leukocyte adhesion receptor PSGL-1. *Immunity* **17**(4)**:** 401-412.

Walker, UA, Tyndall, A, Czirjak, L, Denton, C, Farge-Bancel, D, Kowal-Bielecka, O, Muller-Ladner, U, Bocelli-Tyndall, C, Matucci-Cerinic, M (2007) Clinical risk assessment of organ manifestations in systemic sclerosis: a report from the EULAR Scleroderma Trials And Research group database. *Ann Rheum Dis* **66**(6)**:** 754-763.

Zarbock, A, Ley, K, McEver, RP, Hidalgo, A (2011) Leukocyte ligands for endothelial selectins: specialized glycoconjugates that mediate rolling and signaling under flow. *Blood* **118**(26)**:** 6743-6751.

Figure Legends

FIGURE 1 | CD44 expression in lung and BAL cell populations of WT and PSGL-$1^{-/-}$ mice older than one year. (A) Gating strategy (B) Number of CD44+ cells in the whole lung (total CD44+ lung cells) and number of CD45+ and CD45- cells in the CD44+ lung population of aged WT and PSGL-$1^{-/-}$ mice. (C) CD44 expression level (MFI: mean fluorescence intensity) of the whole CD44+ population and the CD44+CD45+ and CD44+CD45- lung subsets of WT and PSGL-$1^{-/-}$ mice. (D) Number of epithelial

cells (EpCAM+), endothelial (CD31+) cells, and fibroblasts (CD90.2+) in the CD44+ lung population of WT and PSGL-1$^{-/-}$ mice (E) CD44 expression level of CD44+ epithelial cells, CD44+ endothelial cells and CD44+ fibroblasts present in the lungs of WT and PSGL-1$^{-/-}$ mice. (F) Number of CD44+ cells in the BAL (total CD44+ cells) of WT and PSGL-1$^{-/-}$ mice, and number of CD45+ and CD45- cells in the CD44+ BAL population of aged WT and PSGL-1$^{-/-}$ mice. (G) CD44 expression level of the CD44+ population and the CD44+CD45+ and CD44+CD45- subsets. (H) Number of epithelial cells (EpCAM+), endothelial (CD31+) cells, and fibroblasts (CD90.2+) in the XΔ44+ BAL population of WT and PSGL-1$^{-/-}$ mice (I) CD44 expression level of CD44+epithelial cells and CD44+ fibroblasts present in the BAL of WT and PSGL-1$^{-/-}$ mice. Lungs: n=11. BAL: n=12. $p<0.05$ by Mann Whitney one-tailed test. Lines and error bars show the mean ± SEM, respectively. Dots represent individual animals.

FIGURE 2 | Characterisation of myeloid and CD45- BAL cell populations in aged WT mice and PSGL-1$^{-/-}$ control and treated mice. (A) Gating strategy for the identification of CD45- and myeloid immune cell populations in the BAL. (B-F) Total numbers of different myeloid immune cell populations present in the BAL of untreated aged WT and PSGL-1$^{-/-}$ mice as well as PSGL-1$^{-/-}$ mice treated with empty LipHA and LipHA+Ev . B) CD45+ cells; C) alveolar macrophages (AM); D) dendritic cells (DC); E) interstitial macrophages (IM); F) eosinophils (Eos). (G) Total number of CD45- BAL cells in untreated aged WT and PSGL1$^{-/-}$ mice as well as in LipHA and LipHA+Ev treated mice. (WT: n=30; PSGL-1$^{-/-}$: n=33; LipHA: n=22, except Eos with n=12, LipHA+Ev: n=21, except Eos with n=12). *$p<0.05$, **$p<0.01$, ***$p<0.001$ by Mann Whitney one-tailed test. Dots represent individual animals. Lines and error bars show

the mean ± SEM, respectively. Three independent experiments were performed with LipHA and LipHA+Ev treatment.

FIGURE 3 | Characterisation of lymphoid BAL cell populations and neutrophils (Gr1+) in WT mice and control and treated PSGL-$1^{-/-}$ mice. (A) Gating strategy for the identification of immune cell subpopulations in the BAL. (B-D) Absolute numbers of lymphoid immune cell populations and neutrophils present in the BAL of WT mice and PSGL-$1^{-/-}$ mice, untreated or treated with LipHA and LipHA+Ev. Gr1: neutrophils. (WT: n=30; PSGL-$1^{-/-}$: n=33; LipHA: n=22 in T cells and n=12 in Gr1 and NK cells, LipHA+Ev: n=21 in T cells and n=12 in Gr1 and NK cells). *$p<0.05$, **$p<0.01$, ***$p<0.001$ by Mann Whitney one-tailed test. Dots represent individual animals. Lines and error bars show the mean ± SEM, respectively. Three independent experiments were performed with LipHA and LipHA+Ev treatment.

FIGURE 4 | Evaluation of PSGL-$1^{-/-}$ mice lung inflammation after treatment with LipHA+Ev. (A) Aged untreated WT and PSGL-$1^{-/-}$ mice and PSGL-$1^{-/-}$ mice treated with LipHA or LipHA+Ev, were evaluated for the presence of interstitial inflammation. Left panels show the lung injury score (0: No disease; 1: Mild; 2: Moderate; 3: Severe). Right panels show the number of animals with no disease, mild, moderate or severe lung lesions and the percentage of animals with absence of disease. (B) Representative images of H&E stained lung sections. (C) Immunohistochemistry images of mouse lungs stained with antibody against CD45. Lines and error bars show the mean ± SEM, respectively. Dots represent individual animals. n=10 in WT group and n=12 in PSGL-$1^{-/-}$ groups. **$p<0.01$ by Mann Whitney one-tailed test. Lungs from mice of two different experiments were histologically analysed.

FIGURE 5 | Evaluation of PSGL-1$^{-/-}$ mice lung fibrosis after treatment with LipHA+Ev. Aged untreated WT and PSGL-1$^{-/-}$ mice and PSGL-1$^{-/-}$ mice treated with LipHA and LipHA+Ev, were evaluated for the presence of interstitial fibrosis (A) and peribronchial fibrosis (B). Upper panels show the lung injury score (0: No disease; 1: Mild; 2: Moderate; 3: Severe). Lower panels show the number of animals with each score and the percentage of animals with absence of disease. (C) Representative images of Masson's trichrome stained mice lungs sections. (D) Representative images of lung sections stained by immunohistochemistry with anti-collagen I antibody. Lines and error bars show the mean ± SEM, respectively. Dots represent individual animals. n=10 in WT group and n=12 in PSGL-1$^{-/-}$ groups. *$p<0.05$ by Mann Whitney one-tailed test. Lungs from mice of two different experiments were histologically analysed.

FIGURE 6 | Cytokine expression in BAL cells of aged untreated WT and PSGL-1$^{-/-}$ mice and PSGL-1$^{-/-}$ mice treated with LipHA and LipHA+Ev. (A-C) Absolute number of CD45+ BAL cell populations producing IFN-γ (A), IL-6 (B) and IL-10 (C). (D-E) Absolute number of CD45- BAL cell populations producing IL-6 (D) and IL-17-A (E) (WT: n=8-14; PSGL-1$^{-/-}$: n=10-21; LipHA: n=10-12; LipHA+Ev: n=9-12). *$p<0.05$, **$p<0.01$, ***$p<0.001$ by Mann Whitney one-tailed test. Lines and error bars show the mean ± SEM, respectively. Dots represent individual animals.

FIGURE 7 | Evaluation of everolimus effect in the presence of BAL myofibroblast and apoptosis in lungs. (A) Absolute number of myofibroblast present in BAL of different experimental groups (untreated WT and PSGL-1$^{-/-}$: n=21; PSGL-1$^{-/-}$ treated with LipHA: n=10 or LipHA+Ev: n=9). (B) Representative images of lung apoptosis assessed by Caspase 3 immunohistochemistry (IHQ). (C) Quantification of Caspase3+ cells in IHQ-stained lung sections of different experimental groups (WT: n=2; PSGL-1$^{-/-}$ mice: n=5). (D) Absolute numbers of CD45+ and CD45- Annexin V+ cells in lungs of

WT and PSGL-1$^{-/-}$ mice. (E) Number of endothelial cells, epithelial cells and fibroblasts expressing Annexin V in the lungs of WT and PSGL-1 KO mice (n= 12). **p<0.01, ***p<0.001 by Mann Whitney one-tailed test. Lines and error bars show the mean ± SEM, respectively. Dots represent individual animals.

SUPPLEMENTARY FIGURE 1 | (A) Treatment schedule followed to treat aged PSGL-1$^{-/-}$ mice with LipHA and LipHA+Ev. (A) X-ray images before and after intratracheal administration of Iopamiro 300® contrast medium. (B) Representative images of lung tissue sections stained by H&E after contrast medium administration.

SUPPLEMENTARY TABLE I. Flow cytometry antibodies and reagents used for the characterization of murine lung and BAL cells and cytokines.

SUPPLEMENTARY FIGURE 2

Characterisation of CD45+ and CD45- BAL cell populations in aged PSGL-1$^{-/-}$ untreated (NT, n=32) and after intratracheal treatment with water (n=7).

FIGURES

Figure 1

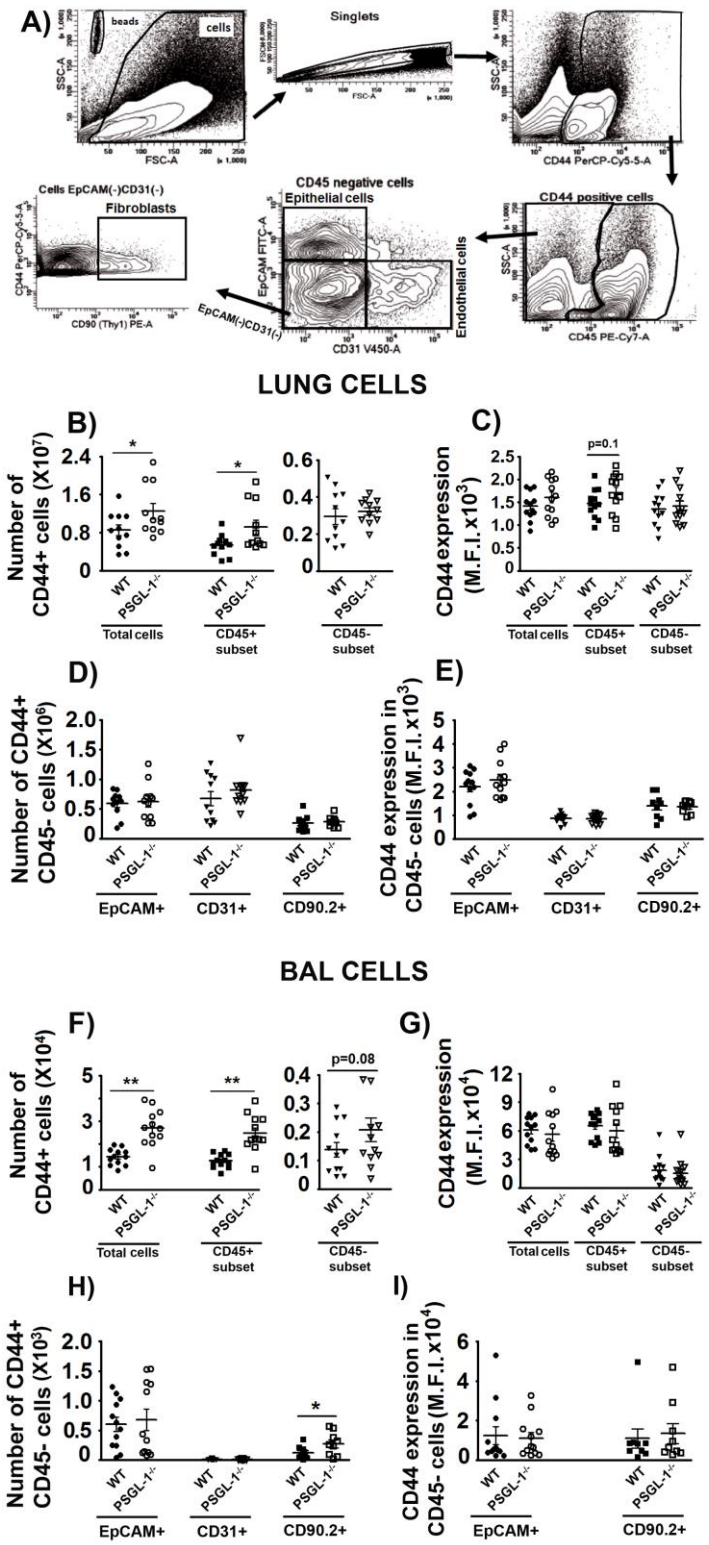

Figure 2

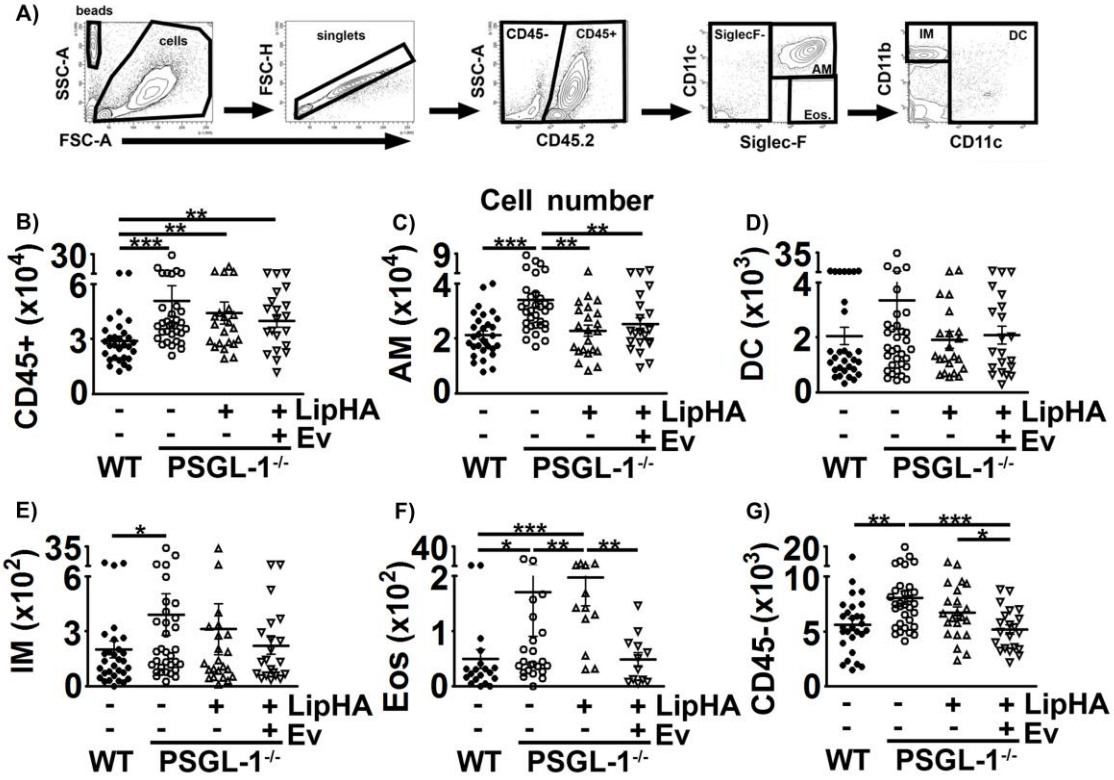

Figure 3

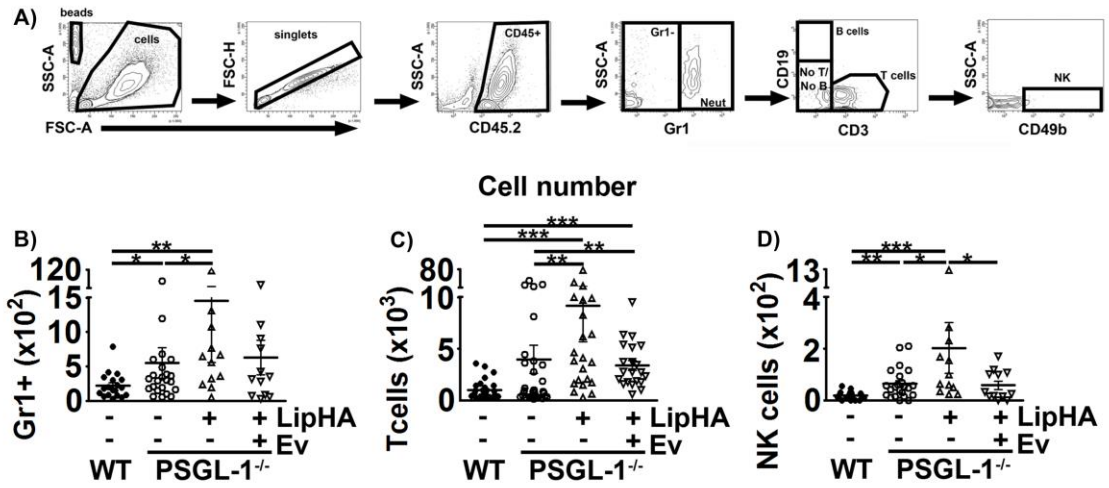

Figure 4

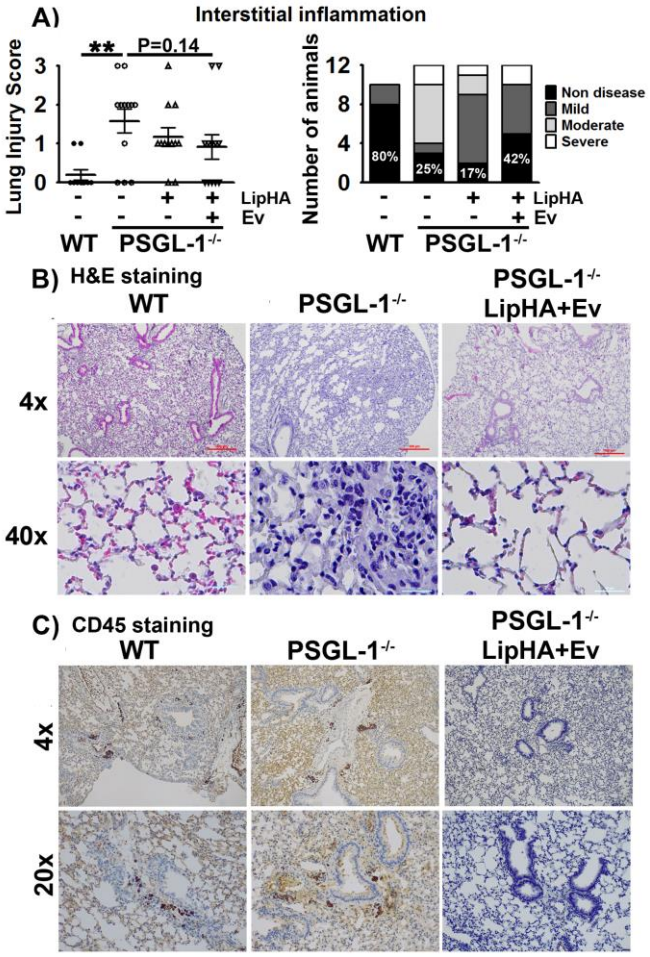
A)
Interstitial inflammation
Lung Injury Score
**
P=0.14
3
2
1
0
LipHA
Ev
WT
PSGL-1-/-
Number of animals
12
8
4
0
80%
25%
17%
42%
Non disease
Mild
Moderate
Severe
B) H&E staining
WT
PSGL-1-/-
PSGL-1-/-
LipHA+Ev
4x
40x
C) CD45 staining
WT
PSGL-1-/-
PSGL-1-/-
LipHA+Ev
4x
20x

Figure 5

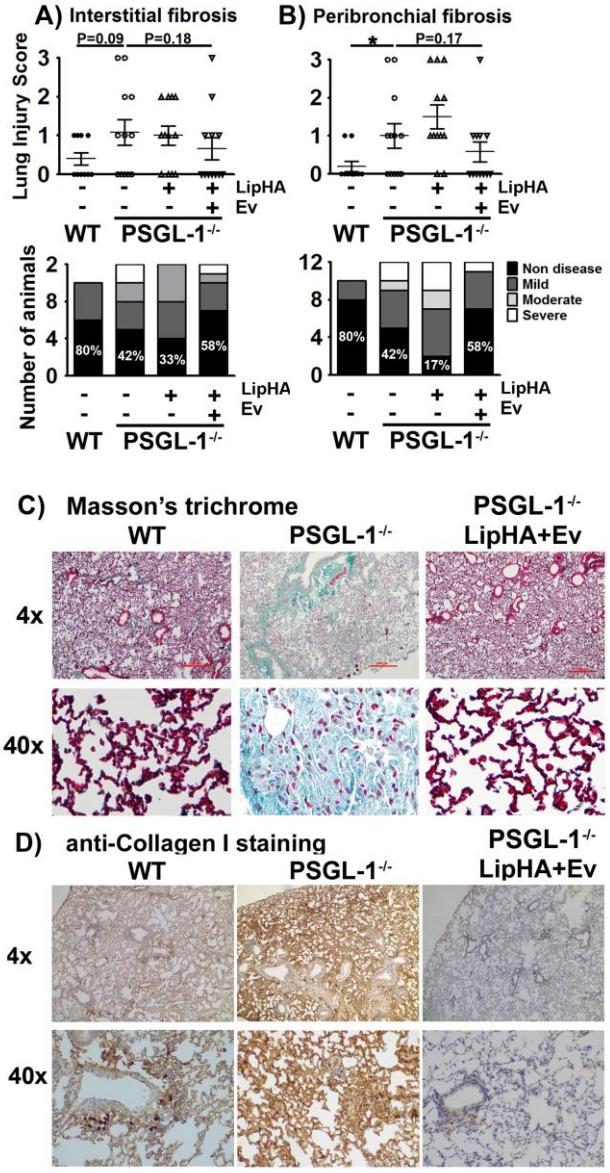
A) Interstitial fibrosis
P=0.09
P=0.18
Lung Injury Score
LipHA
Ev
WT
PSGL-1-/-
Number of animals
80%
42%
33%
58%
B) Peribronchial fibrosis
*
P=0.17
80%
42%
17%
58%
Non disease
Mild
Moderate
Severe
C) Masson's trichrome
WT
PSGL-1-/-
PSGL-1-/- LipHA+Ev
4x
40x
D) anti-Collagen I staining
WT
PSGL-1-/-
PSGL-1-/- LipHA+Ev
4x
40x

Figure 6

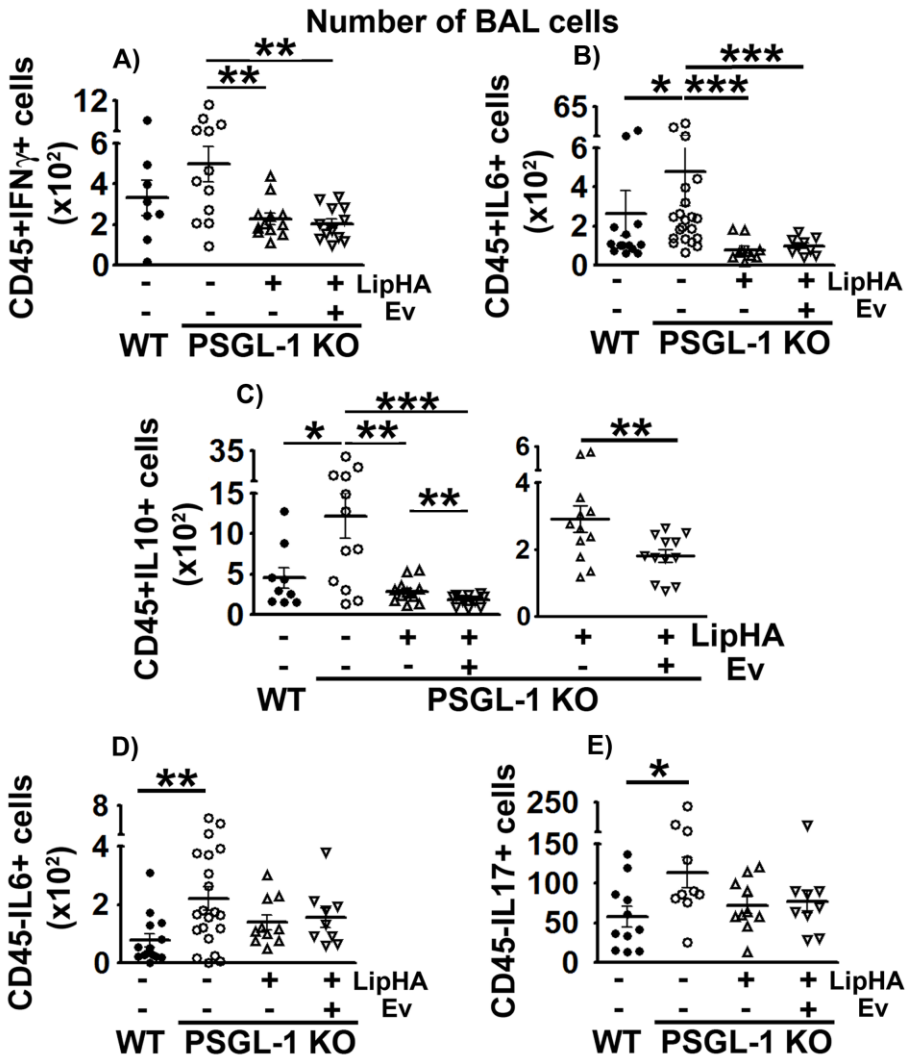
Number of BAL cells
A)
B)
C)
D)
E)
CD45+IFNγ+ cells (x10²)
CD45+IL6+ cells (x10²)
CD45+IL10+ cells (x10²)
CD45-IL6+ cells (x10²)
CD45-IL17+ cells
LipHA
Ev
WT
PSGL-1 KO

Figure 7

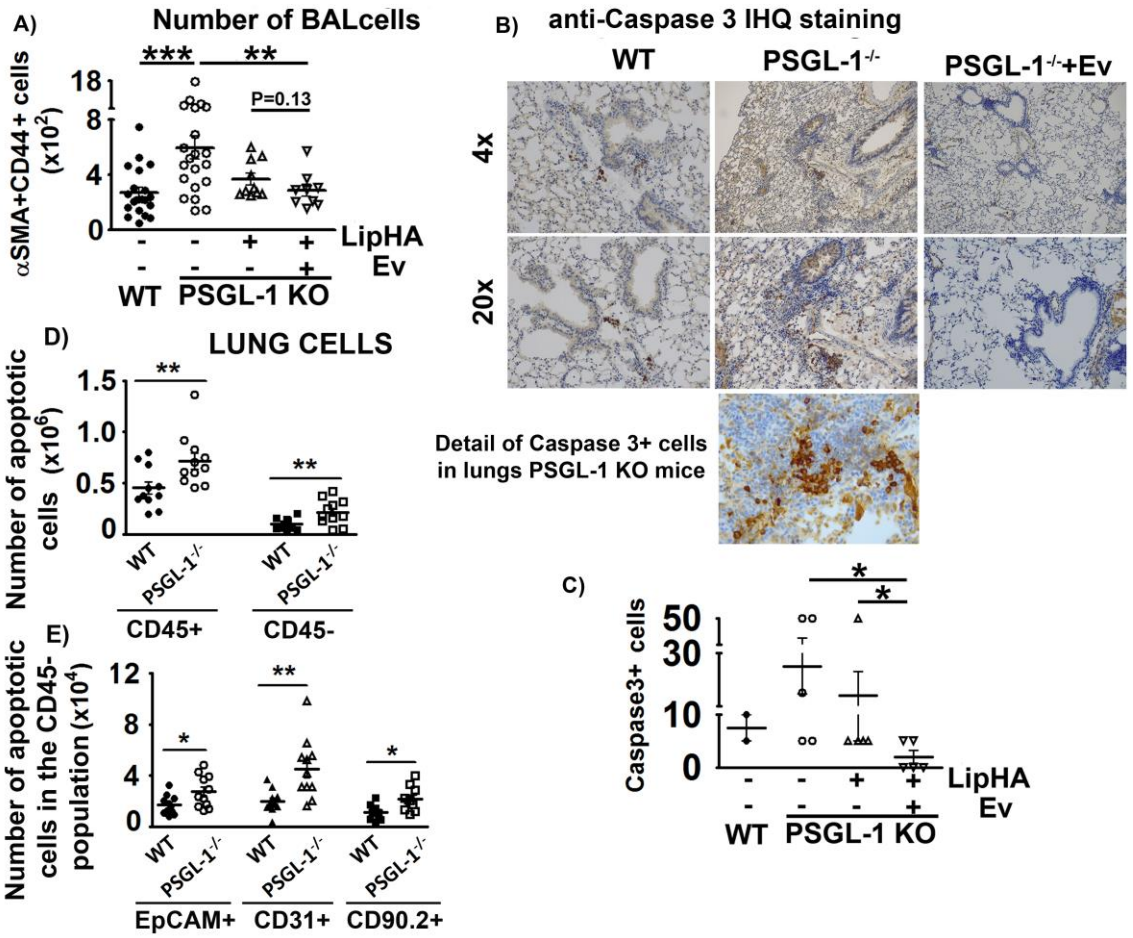
A)
Number of BALcells
αSMA+CD44+ cells (x10²)
***
**
P=0.13
LipHA
Ev
WT
PSGL-1 KO
B)
anti-Caspase 3 IHQ staining
WT
PSGL-1-/-
PSGL-1-/-+Ev
4x
20x
Detail of Caspase 3+ cells in lungs PSGL-1 KO mice
C)
Caspase3+ cells
LipHA
Ev
WT
PSGL-1 KO
D)
LUNG CELLS
Number of apoptotic cells (x10⁶)
CD45+
CD45-
E)
Number of apoptotic cells in the CD45- population (x10⁴)
EpCAM+
CD31+
CD90.2+

Supplem Figure 1

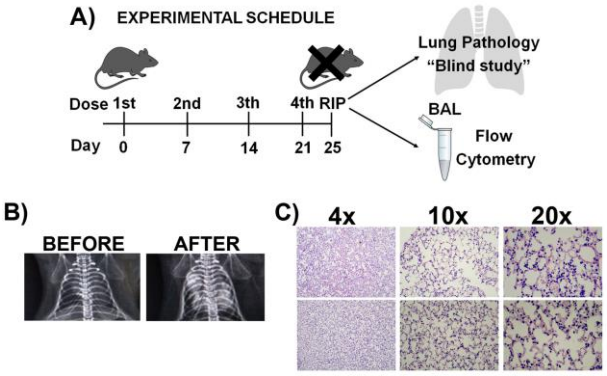

Supplem Figure 2

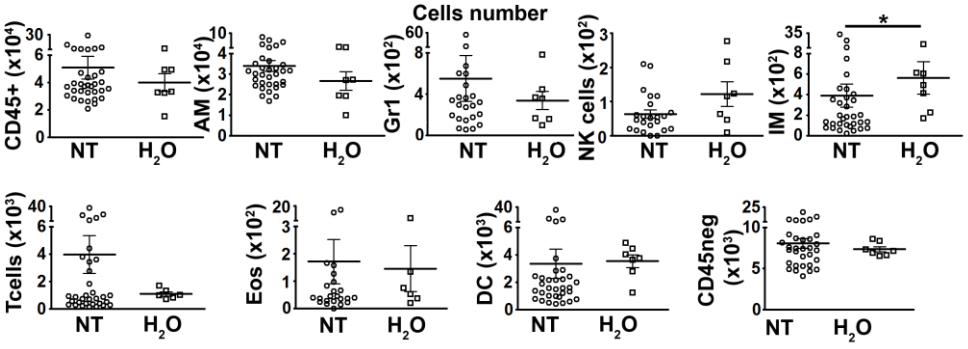

SUPPLEMENTARY TABLE I

Target	Fluorochrome	Dilution	Company	Reference
CD45	BV421	1:100	BD Horizon	562895
Ly-6G, Ly-6C	APC	1:100	BD Pharmingen	553129
CD3	PE-Cy7	1:50	Invitrogen	25-0031-82
CD19	FITC	1:25	Immunotools	22220193
CD49b	APC-Vio770	1:25	BD Pharmingen	553858
Siglec-F	PE	1:100	BD Pharmingen	552126
CD11c	PE-Cy7	1:50	Invitrogen	25-0114-82
CD11b	FITC	1:50	BD Pharmingen	553310
CD44	APC	1:50	Miltenyi	130-102-563

IL-10	PerCP-Cy5.5	1:50	BioLegend	505028
IFN-γ	APC	1:25	Miltenyi	130-102-340
IL-17A	PerCP-Cy5.5	1:50	BD Pharmingen	560666
IL-6	APC	1:50	Miltenyi	130-102-401
α-SMA	Alexa Fluor 488	1:50	Invitrogen	53-9760-80
EpCAM (CD326)	FITC	1:50	Miltenyi Biotec	130-123-674
CD31	BV421	1:100	BD Horizon	563356
CD90.2 (Thy1.2)	PE	1:50	Miltenyi Biotec	130-102-489
CD44	perCp Cy5.5	1:50	Biolegend	103031
CD45.2	PE Vio770	1:100	Miltenyi Biotec	130-125-862
Anexin V	DY634 (alternative APC)	1:100	Inmunostep	ANXVDY-200T